The Interactions between SNAGCU Solder and NI(P)/AU, NI(P)/PD/AU UBMS

Jui-Yun Tsai, Josef Gaida, Gerhard Steinberger and Albrecht Uhlig
Atotech Deutschland GmbH
Berlin, Germany

ABSTRACT

The metallurgical reactions between the Sn3.5Ag0.5Cu solder and two different UBM structures, Ni(P)/Au and Ni(P)/Pd/Au, were studied. Two kinds of Ni(P) layers, medium-P and high-P content, were selected. The reliability of the solder joints were characterized by ball shear test after multiple reflows. It was found that the reaction products at the interface were the same in the all systems after multiple reflows. However, the addition of Pd layer between Ni(P) and Au played strong effects on morphology of compounds and strength of joints as well. The morphology of the compounds were needle-shaped in the Ni(P)/Au system and were layer-shaped in the Ni(P)/Pd/Au system. The needle-shaped compounds became the weak points during the ball shear test. Therefore, the major fracture mode of ball shear test was between the roots of needle-shaped compounds and Ni(P)/Au UBMs. In the Ni(P)/Pd/Au system, the major fracture mode was inside the solder. The thickness of Ni_3P in high-P content Ni(P) layer is thicker than that in medium-P content Ni(P) layer.

Keyords: Ni(P)/Pd/Au, Ni(P)/Au, Pb-free solder, flip-chip technology

INTRODUCTION

Under bump metallization (UBM) is a multilayer structure and an essential part of low-cost solder flip-chip technology. The functions of UBM include adhesion to the terminal electrode, diffusion barrier between solder and terminal electrodes and wetting ability for soldering. Intermetallic compounds will form at the UBM/solder interface during assembly process. The formation of thin intermetallic compound layer provides good metallurgical bond between UBM and solder. The growth of intermetallic compounds have been found to be minimized in the case of Ni UBM, as the reaction between Ni and Sn is much slower than between Cu and Sn [1]. Electroless Ni(P)/immersion Au layer has been considered as a promising UBM due to its many advantages such as good diffusion barrier against solder, excellent selective deposition, and low cost as compared to thin-film vacuum processes [2-3]. However, the well known issue “black pad” has been concerned when electroless Ni(P)/ immersion Au was used. It has been identified that the hyper corrosive activity of immersion Au process on the near Ni surface [4]. One possible alternative solution is an electroless Ni(P)/electroless Pd/immersion Au system. The Pd layer between Au and Ni can prevent Ni from corrosion attacked by immersion Au process.

We also confirmed that the outer layer Au in Ni(P)/Au UBM can no longer prevent Ni diffusing out to the Au surface after thermal aging by Auger Electron Spectroscopy (AES) analysis, as shown in Fig. 1(a). The out-diffusion of Ni could be oxidized and cause the problems of solderability or wire bondability during bonding process. In contrast, there is no Ni element can be detected after thermal aging Ni(P)/Pd/Au system, as shown in Fig. 1(b). Therefore, the advantage of Pd layer is not only used as a sacrificial layer to prevent corrosion of Ni during immersion Au plating, but also as a diffusion barrier for Ni out-diffusion before bonding process.

The interfacial reactions between Pb-free solders and UBMs play a crucial point due to both high Sn content and high reflowing temperature [5-6]. Therefore, the first objective of this study is to investigate the difference of interfacial reaction between Pb-free solder and Ni(P)/Au UBM, and Pb-free solder and Ni(P)/Pd/Au UBM. The second objective is to investigate the effect of different UBM on the reliability of solder joint after multiple reflows.

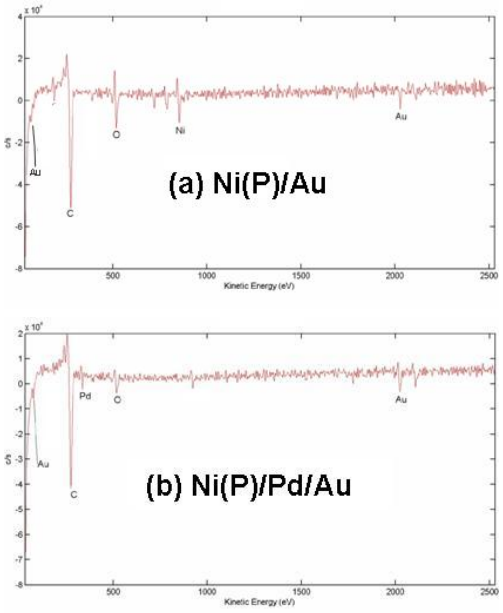

Fig. 1 Auger Electron Spectroscopy (AES) analysis of (a) Ni(P)/Au (4.6 μm / 100 nm) UBM and (b) Ni(P)/Pd/Au (4.6 μm / 200 nm / 30 nm) UBM after aging at 175 ^{o}C for 16 hrs.

EXPERIMENTAL PROCEDURE

The spalling of intermetallic compounds, which seriously affects the solder joint reliability, was found in the Ni-P metallization [7-10]. Sohn et al. reported the increase in the intermetallic compounds with the P-content in Ni(P) layer [7]. Therefore, there are two different P content of Ni(P) layers were used in this study. Four different UBMs were investigated in this study. Table 1 shows layer structure and thickness of Ni(P)/Au and Ni(P)/Pd/Au UBMs. Each UBM was deposited on 300 μm diameter of AlCu alloy pads on 6-inch wafer. After deposition of UBMs, pre-formed 300μm Sn3.5Ag0.5Cu solder balls were placed on the UBM by using resin type flux and immediately followed by reflowing with profile as shown in Fig. 2. The numbers of reflow cycle test are 1, 5 and 10.

After reflowing, the solder joints were metallographiccally polished to reveal the interface and the internal microstructure. In order to reveal morphologies of intermetallic compounds, the samples were etched with a 5 vol.% HCl (in methanol) solution for a few seconds. They were examined by scanning electro microscopy (SEM) and by energy dispersive X-ray spectroscopy (EDX). The ball shear strength of 30 solder joints with four different UBMs after reflow cycle tests were measured using the Dages Series 4000 Bond Tester. The shear speed is 200 μm m/s and shear height is 10 nm. 30 solder balls were sheared to obtain the average and the extent deviation.

Table 1. Layer structure and thickness of the UBMs

UBM	Thickness	P-content
medium-P Ni(P)/Au	4.6μm/100nm	6~7%
high-P Ni(P)/Au	4.4μm/100nm	8~9%
medium-P Ni(P)/Pd/Au	4.6μm/200nm/30nm	6~7%
high-P Ni(P)/Pd/Au	4.4μm/200nm/30nm	8~9%

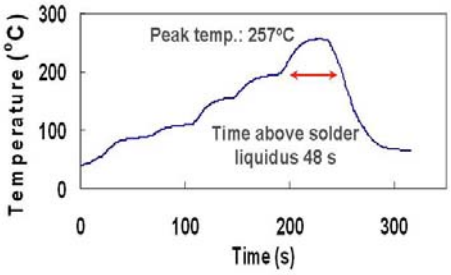

Fig. 2. Reflow profile for Sn3.5Ag0.5Cu

RESULTS and DISCUSSIONS

A. The Interfacial Reactions between SnAgCu Solder and Ni(P)/Au

Fig. 3 shows the SEM cross-sectional images of solder joints between Sn3.5Ag0.5Cu solder and medium-P Ni(P)/Au substrates for 1, 5 and 10 reflow cycles. After first reflow, the thin Au layer dissolved into liquid solder rapidly and a Cu-Ni-Sn ternary compound layer was formed at the liquid solder/Ni(P) interface, as shown in Fig. 3(a). According to EDX analysis, the relative atomic ratio of Cu:Ni:Sn is 31:21:48, which corresponds to $(Cu,Ni)_6Sn_5$. In addition, a typical P-rich phase, Ni_3P crystalline compound layer was observed between $(Cu,Ni)_6Sn_5$ compound and Ni(P) substrates. As can be seen in Fig. 3(a), the $(Cu,Ni)_6Sn_5$ compounds revealed the needle-shaped microstructures after initial reflow. Fig. 4(a) shows the top-view for the morphology of needle-shaped $(Cu,Ni)_6Sn_5$, which included a lot of channels between compound grains.

When the reflow cycle increased to 5 times, the $(Cu,Ni)_6Sn_5$ grew thicker and some $(Ni,Cu)_3Sn_4$ compounds mixed with $(Cu,Ni)_6Sn_5$ can be detected, as shown in Fig. 3(b). Moreover, there were voids occurred within the $(Cu,Ni)_6Sn_5$/$(Ni,Cu)_3Sn_4$ mixing compounds, see Fig. 3(c). The possible reason of voids formation is that the needle-shaped compounds provide many diffusion channels for the liquid Sn to directly react with Ni(P) to form the $(Cu,Ni)_6Sn_5$/$(Ni,Cu)_3Sn_4$ mixing compounds during reflowing. As a result, the liquid Sn was easily trapped in the loose mixing compound layers during cooling down and the voids were shown after etching process. The thickness of Ni_3P crystalline layer increased significantly as reflow time increased, which indicated the Ni was depleted continuously from Ni(P). The thickness of Ni_3P is 0.49 μm after 10 reflow cycles.

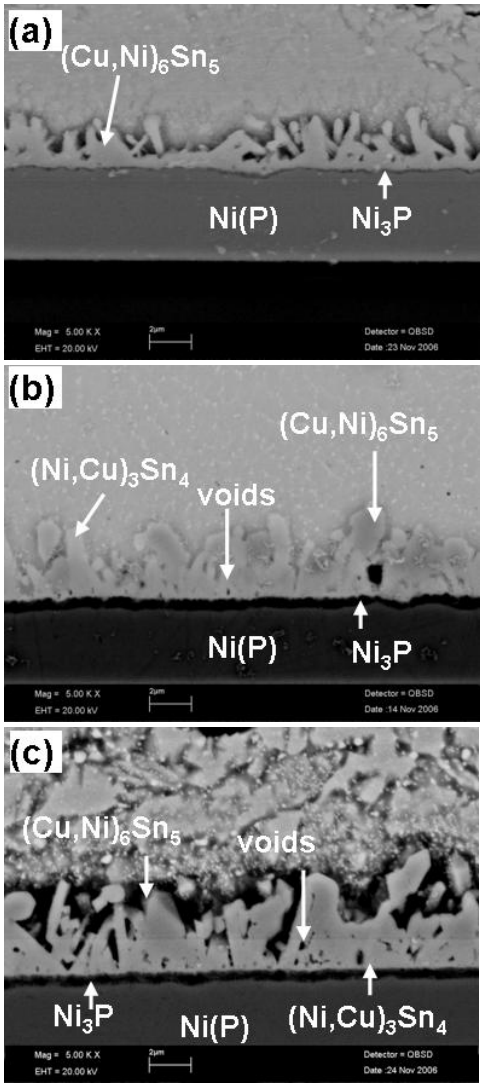

Fig. 3: SEM images of Sn3.5Ag0.5Cu/medium-P Ni(P)/Au interfaces after (a) 1, (b) 5 and (c) reflow cycles.

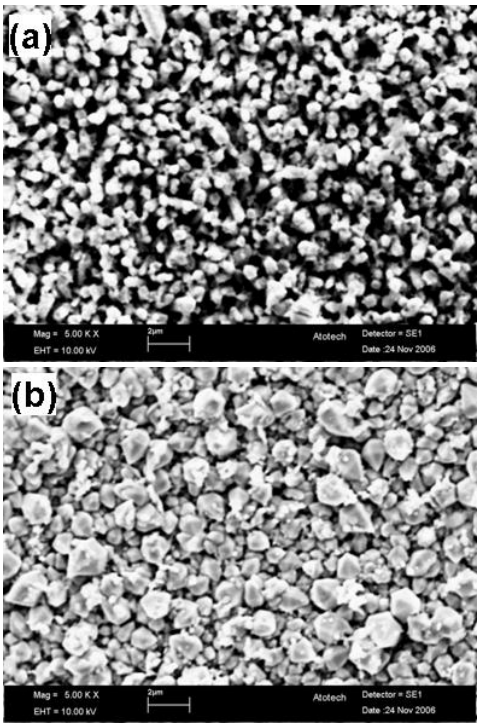

Fig. 4: SEM image showing the top view of (a) $(Cu,Ni)_6Sn_5$/$(Ni,Cu)_3Sn_4$ mixing compounds on Ni(P)/Au, (b) $(Cu,Ni,Pd)_6Sn_5$ compounds on Ni(P)/Pd/Au after one reflow cycle. The solder was removed with 30% nitric acid.

In case of high-P Ni(P)/Au UBMs, the results of interactions between solder and UBMs were the same as that of medium-P Ni(P)/Au UBMs, as shown in Fig. 5(a)–(c). The Ni_3P phase grew thicker with increasing of the reflow time. The thickness of Ni_3P is 0.52 μm after 10 reflow cycles.

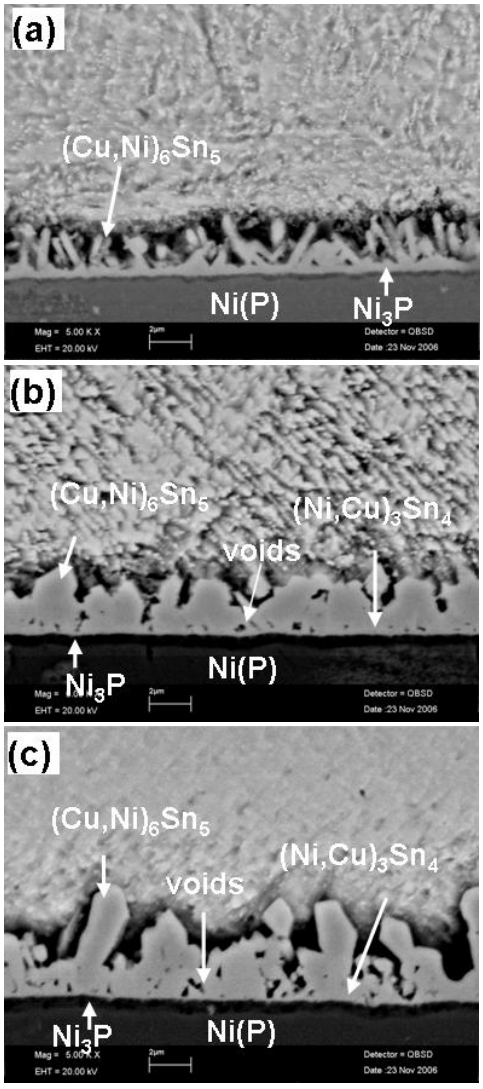

Fig. 5 SEM images of Sn3.5Ag0.5Cu/high-P Ni(P)/Au interfaces after (a) 1, (b) 5 and (c) 10 reflow cycles.

B. The Interfacial Reactions between SnAgCu Solder and Ni(P)/Pd/Au

Fig. 6(a)-(c) show the SEM cross-sectional images of solder joints between Sn3.5Ag0.5Cu solder and medium-P Ni(P)/Pd/Au substrates for 1, 5 and 10 reflow cycles. After first reflow, the interfacial compound layers were determined to be $(Cu,Ni)_6Sn_5$ dissolved with a little amount of Pd, as shown in Fig. 6(a). The respect atomic ratio of Cu:Ni:Pd:Sn is 34:18:1:47 by EDX analysis, which is similar to $(Cu,Ni,Pd)_6Sn_5$ configuration with Ni and Pd atoms substituted for Cu sublattices [11]. In addition, no any $PdSn_4$ phase can be found at the interface or inside solder bumps. It is believed that the thin Pd layer will be completely dissolved into solder right after Au dissolution and allows liquid solder to react with the Ni(P) substrates. From the literature, the saturated solubility of Pd in the SnAg solder at 250 ^{o}C is around 0.045 mole fraction [12]. In this study, if the 200 nm Pd layer was dissolved completely into liquid solder, the solubility of Pd in the solder joint is still lower than the value mentioned above. Therefore, the reason of no observation of $PdSn_4$ might be due to the low Pd concentration in the solder. It is interesting to note that the inserted Pd layer not only changed the composition but also the morphology of the interfacial compound layer. It was more layer-type (Fig. 6(a)-(c)) than that of Ni(P)/Au. Fig. 4(b) is a top-view image showing the morphology of $(Cu,Ni,Pd)_6Sn_5$, which revealed the fine space between grains and larger grain size than that in case of Ni(P)/Au system.

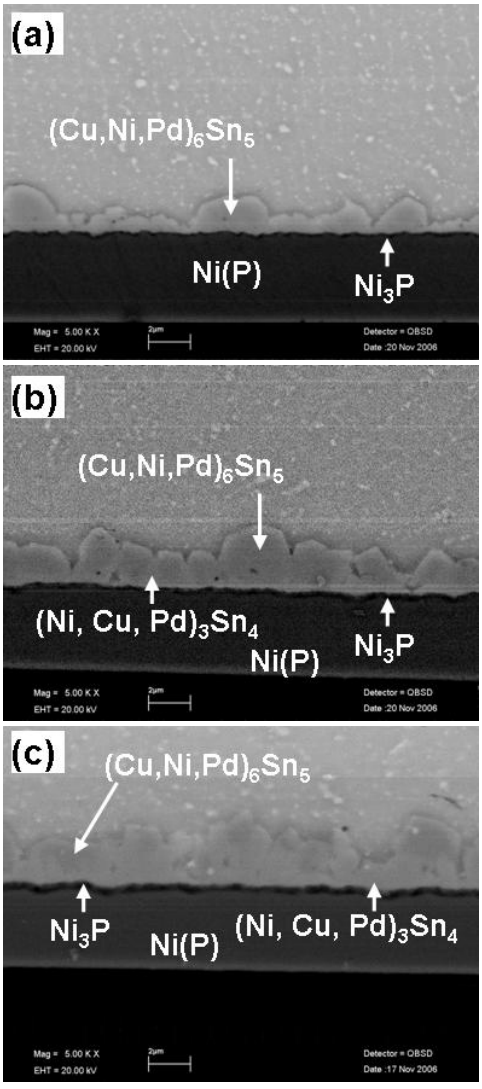

Fig. 6: SEM images of Sn3.5Ag0.5Cu/medium-P Ni(P)/Pd/Au interfaces after (a) 1, (b) 5 and (c) 10 reflow cycles.

It has been reported that the morphology of Cu_6Sn_5 grains highly depends on the interfacial energy, $\gamma_{solder/Cu6Sn5}$, between the molten solder and Cu_6Sn_5 grains [13]. From the thermodynamic aspect, higher $\gamma_{solder/Cu6Sn5}$ would promote the formation of semi-spherical Cu_6Sn_5 grains to minimize the total interfacial area between the molten solder and Cu_6Sn_5 grains. On the contrary, the low $\gamma_{solder/Cu6Sn5}$ would promote irregular or facet morphology of Cu_6Sn_5 compound grains. The dissolved Pt atoms in Sn can change the interfacial energy, $\gamma_{solder/Cu6Sn5}$, on Cu substrate and then prompt irregular Cu_6Sn_5grains [14]. In order to have better understanding of the Pd effect on the morphology of interfacial compound layer, the interaction between Sn3.5Ag0.5Cu solder doped 0.15wt.% Pd and Ni(P)/Au layer at 250 °C for 2 reflow cycles was studied, as shown in Fig. 7. It can be seen that the $(Cu,Ni,Pd)_6Sn_5$ compounds also had layer-shaped structure. It indicates that a certain amount of Pd in solder will change the morphology of interfacial compounds from needle-shaped to layer-shaped. Therefore, the possibility of changed morphology of $(Cu,Ni,Pd)_6Sn_5$ on Ni(P)/Pd/Au UBM is that the interfacial energy, $\gamma_{solder/Cu6Sn5}$, was changed by the dissolved Pd.

After 5 and 10 reflow cycles, the $(Cu,Ni,Pd)_6Sn_5$ grew coarse and thicker with increasing of the reflow time, as shown in Fig. 6(b) and (c). In addition, a layer underneath $(Cu,Ni,Pd)_6Sn_5$ was determined as $(Ni,Cu,Pd)_3Sn_4$, the atomic ratio of Cu:Ni:Pd:Sn is 12:30:2:56 by EDX. The Ni_3P phase grew thicker with increasing the reflow time and its thickness is 0.45 μm after 10 reflow cycles.

In case of high-P Ni(P)/Pd/Au UBM structure, the microstructure of interface and reaction products were the same as that of medium-P Ni(P) by SEM and EDX measurement, see Fig. 8(a)-(c). It means that the high-P Ni(P) layer had no significant effect on the interfacial compound layer. However, as shown in Fig. 8 (c), the thickness of Ni_3P phase is thicker (0.62 μm) than that in the medium-P Ni(P)/Pd/Au after 10 reflow cycles.

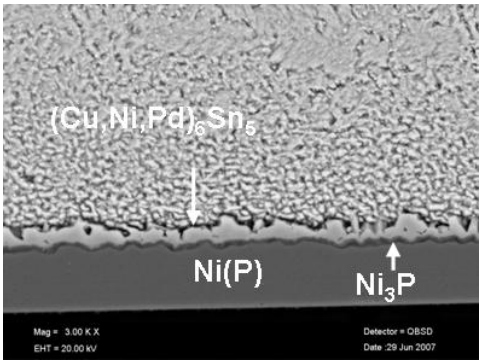

Fig. 7: SEM image of compound morphology between Sn3.5Ag0.5Cu doped with 0.15wt.% Pd and Ni(P)/Au after 2 min reflowing at 250 °C.

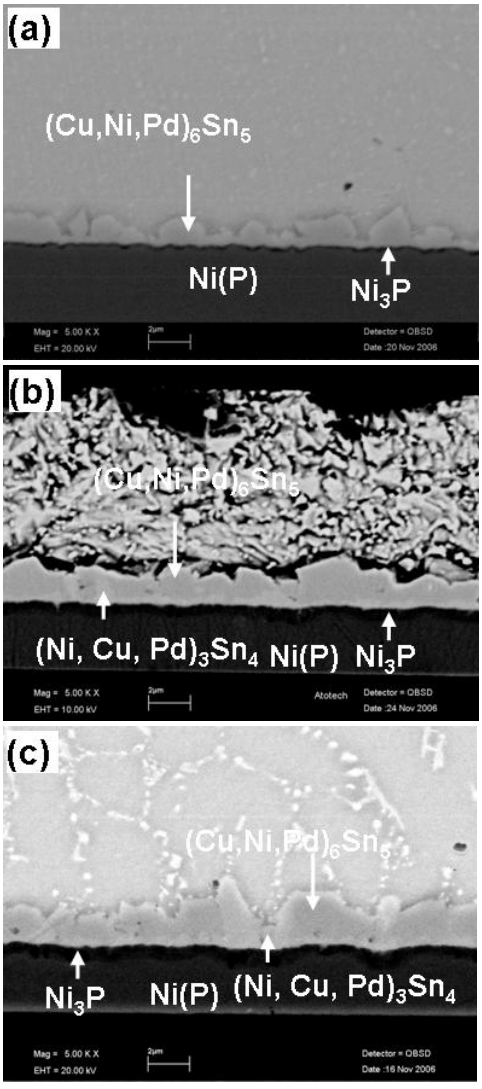

Fig. 8 SEM images of Sn3.5Ag0.5Cu/ high-P Ni(P)/Pd/Au interfaces after (a) 1, (b) 5 and (c) 10 reflow cycles.

C. Solder Ball Shear Test

Ball shear tests were performed to evaluate the effect of the interfacial reactions on the strength of the solder joints as a function of reflow cycles. The variation of average shear strength and standard deviation with respect to four UBMs and different reflow numbers are shown in Figure 9.

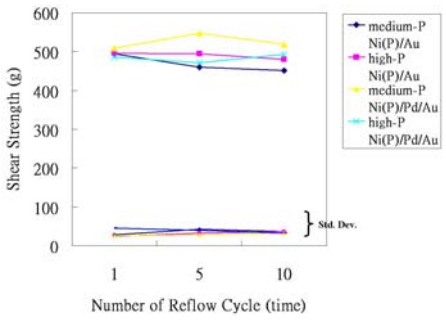

Fig. 9: Shear force of Sn3.5Ag0.5Cu joints with four different UBMs after 1, 5 and 10 reflow cycles.

After 1 reflow cycle, there was no apparent discrepancy in the shear strength was observed between the four different UBMs. Obviously, the Ni(P)/Pd/Au UBMs had better shear strengths compared with Ni(P)/Au UBMs in spite of Ni(P) layer with medium-P or high-P after 10 times of reflow. The observation of fracture mode of soldering on Ni(P)/Au UBM is entirely different from that on Ni(P)/Pd/Au UBM. To further verify the variations of the shear strength of solder joint, the studies of failure surface were conducted by using SEM. Fig. 10(a) and (b) are the SEM images of fracture surfaces in case of Ni(P)/Au, medium-P and high-P Ni(P), respectively, after 1 reflow cycle. Fig. 10(c) and (d) are the enlarged images of Fig. 10(a) and (b), respectively. From the top-view images of fracture surfaces, it can be seen that the fracture surface is broken at $(Cu,Ni)_6Sn_5$ compound and UBM interface. It is due to the less contact area between needle-shaped mixing compounds and UBM, which creates the higher concentration points of stress for crack initiation and results in brittle failure.

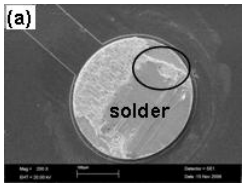

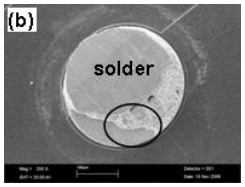

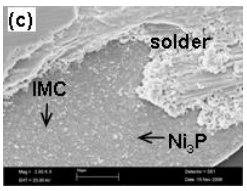

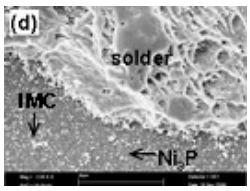

Fig. 10 The fracture surfaces after ball shear tests for Sn3.5Ag0.5Cu/ Ni(P)/Au joints reflowed one time (a) medium-P Ni(P) layer, (b) high-P Ni(P) layer, (c) enlarged image of (a), (d) enlarged image of (b).

After 10 reflow cycles, the mixing compounds became disordered and had void formation at interface, which were discussed in section A. The crack was more easily to initiate between mixing compounds and UBM, as shown in Fig. 11(a) and (b). It is believed to be the key reason that the shear force dropped after 10 reflow cycles.

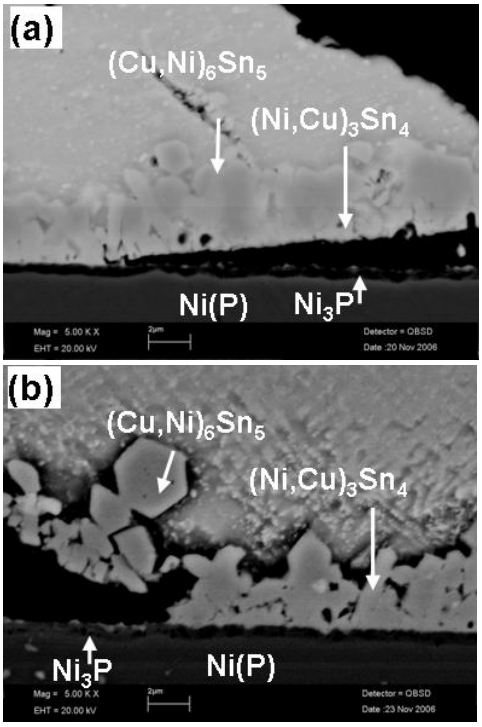

Fig. 11 The fracture surfaces after ball shear tests for Sn3.5Ag0.5Cu/ Ni(P)/Au joints reflowed 10 times (a) medium-P Ni(P) layer, (b) high-P Ni(P) layer.

Fig 12(a) and (b) are the SEM images of fracture surfaces in case of Ni(P)/Pd/Au, medium-P and high-P Ni(P), respectively, after 1 reflow cycle. In contrast to needle-shaped mixing compounds, the layer-shaped structure has better adhesion to the UBM. Therefore, it may increases deformation

energy and prevents brittle fracture between $(Cu,Ni,Pd)_6Sn_5$ compound layers and UBM. Finally, the failure mode was inside the bulk solder after the solder necking and rupture. Fig. 12(c) and (d) show the ductile fracture surfaces of solder for medium-P and high-P Ni(P) of Ni(P)/Pd/Au, respectively. It also means that the shear strength for samples with Ni(P)/Pd/Au were concerned by the strength of the Sn3.5Ag0.5Cu.

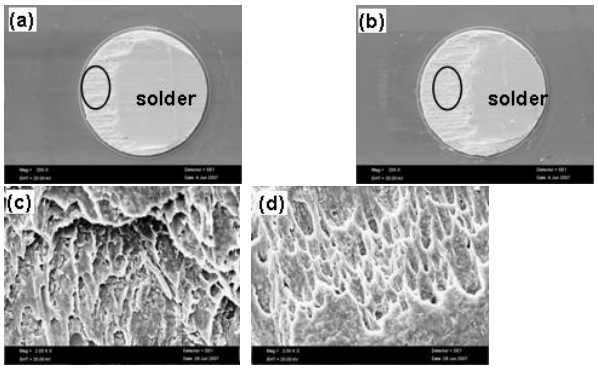

Fig. 12 The fracture surfaces after ball shear tests for Sn3.5Ag0.5Cu/ Ni(P)/Pd/Au joints reflowed 1 time (a) medium-P Ni(P) layer, (b) high-P Ni(P) layer, (c) enlarged ductile fracture of (a), (d) enlarged ductile fracture of (b).

CONCLUSIONS

The addition Pd layer between Ni(P) and Au can change the morphology of intermetallic compounds at interface after soldering. When the interaction is between solder and Ni(P)/Au after soldering, the morphology of imtermetallic compounds at interface is needle-shaped. When the Ni(P)/Pd/Au UBM is used, the intermetallic compounds have layer-shaped. Furthermore, the fracture mode of ball shear test is affected by the microstructure of interfacial intermetallic compounds. Fig. 13 (a) and (b) show the schematic diagram of the interfacial microstructure and fracture surface of Ni(P)/Au UBM after 1 and 10 reflow cycles, respectively. The fracture mode is between imtermetallic compounds and UBM. Fig. 13 (c) and (d) show the schematic diagram of the interfacial microstructure and fracture surface of Ni(P)/Pd/Au UBM after 1 and 10 reflow cycles, respectively. The fracture mode is inside the solder.

The thickness of Ni_3P phase in high-P Ni(P) layer is higher than that in medium-P Ni(P) layer in case of Ni(P)/Au UBM structure and Ni(P)/Pd/Au UBM structure. It was attributed to that the higher P content of Ni(P) was rather easy to form a P-rich layer during the reflow process.

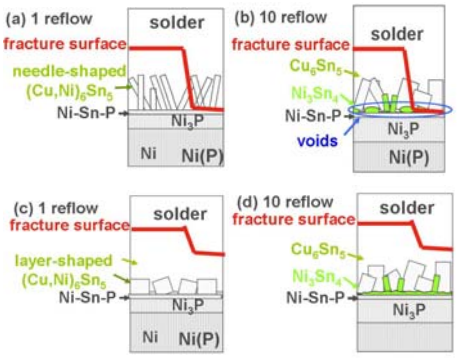

Fig. 13: The schematic diagram of the interfacial microstructure and fracture surface of (a) Ni(P)/Au UBM, 1 reflow cycle (b) Ni(P)/Au UBM, 10 reflow cycles, (ca) Ni(P)/Pd/Au UBM, 1 reflow cycle (b) Ni(P)/Pd/Au UBM, 10 reflow cycles.

REFERENCES

1. K.N. Tu, K. Zeng, Mater. Sci. Eng., R 34, 2001, pp. 1
2. C.Y. Lee, K.L. Lin, Thin Solid Films, V 249, 1994, pp. 201.
3. J.G. Strandjord, S. Popelar, C. Jauernig, Microelectron. Reliab., V 42, 2002, pp. 265.
4. F. D. Bruce Houghton, Future Circuits International, 2000, pp. 121
5. J.W. Jang, D.R. Frear, T.Y. Lee, K.N. Tu, J. Appl. Phys. V 88, 2000, pp. 6359.
6. J.W. Yoon, S.B. Jung, J. Alloys Compd., V 396, 2005, pp. 122.
7. Jang JW, Frear DR, Lee TY, Tu KN. J Appl Phys., V 88, 2000, pp. 6359.
8. Sohn YC, Yu J, Kang SK, Shih DY, Lee TY. J Mater Res., V 19, 2004, pp. 2428.
9. Kim SW, Yoon JW, Jeng SB. J Electron Mater., V 33, 2004, pp. 1182.
10. Yoon JW, Jung SB. J Alloy Compd., V 396, 2005, pp. 122.
11. Ghosh G., J Electron Mater, V29, 2000, pp. 1182.
12. K. Zeng, 6th TRC Austin, TX, October 2003, pp. 27
13. C.Y. Liu, K.N. Tu, J Mater Res, V13, 1998, pp. 1
14. S.J. Wang, C.Y. Liu, Acta Mat. V55, 2007 pp. 3327.